ARID3A knockdown facilitates ferroptosis partly through modulation of the PTEN/Akt pathway in breast cancer

PENGFEI SHI[1*], YAN YI[2*], MAOJIE ZHANG[1], YONGJUN LIU[1], MING JIANG[1] and JIAMING ZHANG[1]

[1]Department of Thyroid and Breast Surgery, The Central Hospital of Wuhan, Tongji Medical College of Huazhong University of Science and Technology, Wuhan, Hubei 430013, P.R. China; [2]Institute of Biomedical Engineering, Union Hospital, Tongji Medical College, Huazhong University of Science and Technology, Wuhan, Hubei 430022, P.R. China

Received August 26, 2025; Accepted May 11, 2026

DOI: 10.3892/ol.2026.15733

Abstract. AT-rich interaction domain 3A (ARID3A) is a tumor regulator that modifies the PTEN and Akt pathway. The present study aimed to investigate the effect of ARID3A knockdown on ferroptosis and the interaction between ARID3A and the PTEN/Akt pathway in breast cancer. Firstly, MCF-7 and MDA-MB-231 cell lines were cultured. Negative control small interfering RNA (siNC) and ARID3A small interfering RNA (siARID3A) were transfected into the cells. Subsequently, siNC, PTEN small interfering RNA (siPTEN) and siARID3A were transfected into the cells alone or in combination. Comprehensive ferroptosis-associated indices were assessed. siARID3A transfection decreased cell viability, mitochondrial membrane potential (MMP) and glutathione peroxidase 4 (GPX4) expression, but increased the levels of malondialdehyde, reactive oxygen species (ROS) and ferrous iron (Fe^{2+}), suggesting that siARID3A transfection promoted ferroptosis. Furthermore, siARID3A transfection upregulated PTEN expression and downregulated phosphorylated (p)-Akt levels, while siPTEN transfection elevated p-Akt levels and attenuated the effect of siARID3A transfection on p-Akt levels, indicating that siARID3A transfection modified the PTEN-mediated Akt pathway. In addition, siPTEN transfection increased cell viability, MMP and GPX4 expression, while decreasing ROS and Fe^{2+} levels. siPTEN transfection weakened the effect of siARID3A transfection on the majority of the aforementioned ferroptosis-associated indices, suggesting that PTEN was implicated in the function of ARID3A in ferroptosis. Overall, ARID3A knockdown promoted ferroptosis partly through modulation of the PTEN/Akt pathway in breast cancer. Despite this, further verification is still needed in future studies.

Correspondence to: Dr Jiaming Zhang, Department of Thyroid and Breast Surgery, The Central Hospital of Wuhan, Tongji Medical College of Huazhong University of Science and Technology, 26 Shengli Street, Wuhan, Hubei 430013, P.R. China
E-mail: zhangjm537@163.com

*Contributed equally

Key words: breast cancer, ferroptosis, AT-rich interaction domain 3A, PTEN, Akt pathway

Introduction

Breast cancer remains the most prevalent cancer type and the most common cause of cancer-associated mortality in women globally, with an estimated 2,295,686 new cases and 665,684 mortalities per year (1). Previous research has uncovered a number of key mechanisms in the tumorigenesis and progression of breast cancer, spanning tumor stemness, intratumoral microbiota and circadian regulation, while artificial intelligence-powered technologies continue to impact early detection and breakthrough therapies advance precision medicine in oncology (2-5).

Ferroptosis is an iron-dependent form of regulated cell death driven by lipid peroxidation, distinct from apoptosis and emerged as an important factor implicated in the pathogenesis and progression of breast cancer, whereby dysregulated iron metabolism and lipid oxidation pathways enhance susceptibility (6,7). Its unique mechanism overcomes resistance to conventional cell death pathways, positioning it as a novel strategic target in breast cancer treatment, especially in triple-negative breast cancer (8,9). Identification of new regulators of ferroptosis may provide potential therapeutic targets for breast cancer treatment.

AT-rich interaction domain 3A (ARID3A), initially identified due to its homology to the embryogenesis-associated dead ringer gene in *Drosophila*, has been implicated in developmental processes, gene regulation and chromatin modification (10). Further attention is being paid to its regulation of carcinogenesis, with an increasing number of studies having been published (11-16). ARID3A has also been reported to promote cell proliferation, migration and invasion in colorectal cancer (11), enhance tumor growth, metastasis and stemness in liver cancer (12), facilitate progression in non-small cell lung cancer (13) and serve as a potential prognostic biomarker for colorectal cancer, cholangiocarcinoma, breast cancer and bladder cancer (11,14-16). Furthermore, ARID3A knockdown may promote ferroptosis to inhibit pancreatic cancer progression and gemcitabine resistance through the targeting of PTEN (17). PTEN is an anti-oncogene and a direct

upstream regulator of the established carcinogenetic Akt pathway (18-21). In addition, PTEN and the Akt pathway are key regulators of ferroptosis in cancer (22-25). Based on the aforementioned findings, it was hypothesized that ARID3A knockdown could facilitate ferroptosis in breast cancer partly through modulation of PTEN/Akt signaling and to the best of our knowledge, this has not yet been reported in previous studies. Therefore, the present study aimed to investigate the effect of ARID3A knockdown on ferroptosis-associated changes and the relationship between ARID3A and PTEN/Akt signaling in breast cancer.

Materials and methods

Cell culture. Breast cancer cell lines MCF-7 (cat. no. iCell-h129) and MDA-MB-231 (cat. no. iCell-h133) were provided by iCell Bioscience, Inc. Minimum Essential Medium (cat. no. G4553; Wuhan Servicebio Technology Co., Ltd.) and DMEM (cat. no. G4511; Wuhan Servicebio Technology Co., Ltd.) supplemented with 10% FBS (cat. no. G8003-500ML; Wuhan Servicebio Technology Co., Ltd.) and penicillin-streptomycin antibiotic solution (cat. no. G4003; Wuhan Servicebio Technology Co., Ltd.) were used for culturing MCF-7 and MDA-MB-231 cells, respectively. Cells were maintained at 37˚C in 5% CO_2. Culture medium was replaced every 2 days and cells were passaged at ~80-90% confluence.

Small interfering RNA (siRNA) transfection. Cells were plated and cultured to 50% confluence. For siRNA transfection, 75 pmol ARID3A siRNA (siARID3A; Shanghai GenePharma Co., Ltd.), PTEN siRNA (siPTEN; Shanghai GenePharma Co., Ltd.) or negative control siRNA (siNC; Shanghai GenePharma Co., Ltd.) were mixed with 15 μl siRNA-Mate Plus Transfection Reagent (cat. no. G04026; Shanghai GenePharma Co., Ltd.) in serum-free medium. After incubation for 15 min to allow mixture formation, cells were incubated with the mixture for 48 h at 37˚C. Cells were then utilized (48 h after transfection) for western blotting and cell viability, malondialdehyde (MDA), reactive oxygen species (ROS), ferrous iron (Fe^{2+}) and mitochondrial membrane potential (MMP) assays. Untransfected cells were cultured as a blank control group. The siRNA sequences (5'-3') were as follows: siNC (sense, UUCUCCGAACGUGUCACGUTT and antisense, ACGUGACACGUUCGGAGAATT), siARID3A (sense, CUCCACAUCUACCUCAAAUTT and antisense, AUUUGAGGUAGAUGUGGAGTT) and siPTEN (sense, UUUGCUACAUUCUAAUGCATT and antisense, UGCAUUAGAAUGUAGCAAATT).

Western blotting. After transfection, cells were incubated with the RIPA lysis buffer (cat. no. G2002; Wuhan Servicebio Technology Co., Ltd.) supplemented with protease and phosphatase inhibitors for 30 min on ice. The lysates were harvested through centrifugation at 12,000 x g for 15 min at 4˚C and total protein was quantified using a BCA Protein Quantitative Detection Kit (cat. no. G2026; Wuhan Servicebio Technology Co., Ltd.). Pre-cast gels (4-20%; cat. no. P06; Shanghai Willget Biotech Co., Ltd.) were used to separate the 20 μg proteins (180 V; 30 min). After polyvinylidene fluoride membrane transfer (300 mA; 1 h), the membranes were blocked with 5% BSA (cat. no. GC305010-25g; Wuhan Servicebio Technology Co., Ltd.) for 30 min at room temperature. Membranes were exposed to primary antibodies, including anti-ARID3A (1:1,000; cat. no. 14068-1-AP; Proteintech Group, Inc.), anti-glutathione peroxidase 4 (GPX4; 1:1,000; cat. no. 30388-1-AP; Proteintech Group, Inc.), anti-phosphorylated (p-)Akt (1:1,000; cat. no. 80455-1-RR; Proteintech Group, Inc.), anti-Akt (1:2,000; cat. no. 10176-2-AP; Proteintech Group, Inc.) and anti-β-actin (1:10,000; cat. no. GB11001; Wuhan Servicebio Technology Co., Ltd.), overnight at 4˚C. Subsequently, membranes were exposed to the HRP-conjugated goat anti-rabbit IgG secondary antibody (1:10,000; cat. no. GB23303; Wuhan Servicebio Technology Co., Ltd.) for 30 min at room temperature. Protein bands were visualized using an ECL kit (cat. no. MA0186; Dalian Meilun Biology Technology Co., Ltd.). The integrated density was assessed using ImageJ (version 1.54; National Institutes of Health).

Cell Counting Kit-8 (CCK-8) assay. Cells were resuspended after transfection, followed by seeding into 96-well plates ($5x10^3$ cells/well). CCK-8 reagent (10 μl; cat. no. G4103; Wuhan Servicebio Technology Co., Ltd.) was added after 24 h of culture, followed by incubation for 2 h at 37˚C. The optical density at 450 nm (OD_{450}) was recorded using a microplate reader (Nanjing Huadong Electronics Group Medical Equipment Co., Ltd.). The relative cell viability was calculated as the OD_{450} of the experimental groups divided by that of the corresponding control groups.

MDA assay. Cells were lysed after transfection and lysate was collected through centrifugation at 12,000 x g for 15 min at 4˚C. The MDA detection solution (cat. no. G4300; Wuhan Servicebio Technology Co., Ltd.) was prepared according to the protocol of the kit. The lysate was added to the MDA detection solution for 40 min at 95˚C. Afterwards, supernatants were collected and utilized for assessment of the optical density at 532 nm (OD_{532}). The relative MDA level was calculated as the ratio of the OD_{532} in the experimental groups to that in the corresponding control groups.

ROS assay. To reach a final concentration of 10 μM, the 2',7'-dichlorofluorescin diacetate probe (ROS Assay Kit; cat. no. S0033; Beyotime Biotechnology) was diluted with staining buffer. After transfection, cells were washed and incubated with probe working solution for 20 min at 37˚C. Staining was analyzed using fluorescence microscopy (Motic China Group Co., Ltd.) and ImageJ (version 1.54; National Institutes of Health). The relative ROS level was calculated as the fluorescence intensity of the experimental groups divided by that of the corresponding control groups.

MMP assay. After transfection, cells were washed with phosphate buffered saline and exposed to MMP staining solution (Enhanced MMP Assay Kit; cat. no. C2003; Beyotime Biotechnology) for 20 min at 37˚C. Fluorescence images were captured (Motic China Group Co., Ltd.) and analyzed using ImageJ (version 1.54; National Institutes of Health). The relative level of aggregates/monomers was calculated as the ratio of aggregates/monomers fluorescence intensity in the experimental groups to that in the corresponding control groups. The

MMP assay was performed to assess mitochondrial functional status under experimental conditions.

Fe^{2+} assay. For the assessment of Fe^{2+} levels, the FerroOrange Fe^{2+} Kit (cat. no. G1727; Wuhan Servicebio Technology Co., Ltd.) was utilized. Briefly, cells were washed with phosphate buffered saline after transfection and exposed to FerroOrange working solution for 30 min at 37˚C in the dark. Following incubation, cells were washed to remove excess probe. Fluorescence images were captured (Motic China Group Co., Ltd.) and the relative Fe^{2+} level was assessed as the fluorescence intensity of the experimental groups divided by that of the corresponding control groups.

Ferrostatin-1 (Fer-1) treatment. To verify whether the observed cell death was ferroptosis-dependent, cells were treated with the ferroptosis inhibitor Fer-1. Briefly, after siNC or siARID3A transfection, cells were treated at 37˚C with Fer-1 (2 μM) for 24 h. Subsequently, CCK-8, MDA, ROS and Fe^{2+} assays were performed as aforementioned.

Statistical analysis. GraphPad Prism (version 9.0; Dotmatics) was utilized for statistical analysis. The results are presented as the mean ± SD. All experiments were performed at least three independent times. Normality was assessed using the Shapiro-Wilk test and homogeneity of variance was evaluated using the Brown-Forsythe test. One-way or two-way ANOVAs with Tukey's multiple comparisons tests were used to compare differences among multiple groups. $P<0.05$ was considered to indicate a statistically significant difference.

Results

ARID3A knockdown promotes ferroptosis in breast cancer cell lines. siARID3A transfection significantly reduced ARID3A expression in MCF-7 and MDA-MB-231 cells, in comparison to the siNC group, suggesting effective transfection (Fig. 1A). siARID3A transfection significantly decreased the viability of MCF-7 and MDA-MB-231 cells in comparison to the siNC group (Fig. 1B), but significantly increased MDA levels (Fig. 1C) and ROS levels (Fig. 1D) in these cell lines. siARID3A transfection significantly enhanced Fe^{2+} levels in MDA-MB-231 cells, in comparison with the siNC group, while no statistically significant change was observed in MCF-7 cells (Fig. 1E). In addition, siARID3A transfection significantly reduced aggregate/monomer expression, which in turn indicated reduced MMP (Fig. 2A), suggesting mitochondrial functional impairment and significantly reduced GPX4 expression (Fig. 2B) in MCF-7 and MDA-MB-231 cells, compared with the siNC group. Furthermore, treatment with Fer-1 partially reversed siARID3A-induced reduction in cell viability and attenuated the increases in MDA, ROS and Fe^{2+} levels, further supporting the involvement of ferroptosis in ARID3A knockdown-induced cell death (Fig. S1).

ARID3A knockdown upregulates PTEN expression and inactivates the Akt pathway in breast cancer cell lines. siARID3A transfection significantly upregulated PTEN expression in MCF-7 cells, while PTEN expression exhibited an increasing trend but did not reach statistical significance in MDA-MB-231 cells. Furthermore, siARID3A transfection significantly downregulated p-Akt levels in both MCF-7 and MDA-MB-231 cells (Fig. 3), suggesting that ARID3A-mediated Akt regulation may differ according to cellular context.

PTEN knockdown activates the Akt pathway in breast cancer cell lines. siPTEN transfection significantly reduced PTEN expression in MCF-7 and MDA-MB-231 cells, in comparison to the siNC group, suggesting effective transfection. Furthermore, siPTEN transfection significantly elevated p-Akt levels in the MCF-7 cell line compared with the siNC, but not in the MDA-MB-231 cell line. However, siPTEN transfection significantly attenuated the inhibitory effect of siARID3A transfection on p-Akt levels in both MCF-7 and MDA-MB-231 cells (Fig. 4), indicating that PTEN remained functionally involved in ARID3A-mediated Akt regulation.

PTEN knockdown attenuates the effect of ARID3A knockdown on ferroptosis in breast cancer cell lines. siPTEN transfection significantly increased the viability of MCF-7 and MDA-MB-231 cells in comparison to the siNC groups (Fig. 5A). However, siPTEN transfection did not significantly alter MDA levels in the MCF-7 and MDA-MB-231 cell lines in comparison with the siNC groups (Fig. 5B). siPTEN transfection significantly reduced ROS levels in the MCF-7 cell line but not in the MDA-MB-231 cell line (Fig. 5C) and significantly decreased Fe^{2+} levels in the MDA-MB-231 cell line but not in the MCF-7 cell line, in comparison with the siNC groups (Fig. 5D). Notably, siPTEN and siARID3A co-transfection significantly increased viability in MCF-7 and MDA-MB-231 cells, significantly reduced MDA levels in MDA-MB-231 cells, and significantly reduced ROS and Fe^{2+} levels in MCF-7 and MDA-MB-231 cells, in comparison with siARID3A group (Fig. 5A-D). In addition, siPTEN transfection significantly elevated aggregate/monomer levels, in turn indicating higher MMP in MDA-MB-231 cells but not in MCF-7 cells (Fig. 6A) and significantly increased GPX4 expression in both MCF-7 and MDA-MB-231 cells in comparison with the siNC groups (Fig. 6B). siPTEN and siARID3A co-transfection significantly increased aggregate/monomer expression, which in turn indicated elevated MMP, and significantly elevated GPX4 expression in MCF-7 and MDA-MB-231 cells compared with the siARID3A group (Fig. 6A and B).

Discussion

ARID3A has been reported to be a regulator of cancer pathogenesis (11-13). A previous study revealed that ARID3A was upregulated in colorectal cancer tissues, promoted colorectal cancer cell proliferation, migration and invasion by elevating aurora kinase A (AURKA) and its higher expression predicted a worse survival in patients with colorectal cancer (11). An additional study reported that ARID3A enhanced tumor growth, metastasis and expression of downstream stemness-associated genes in liver cancer by forming a transcriptional complex with centrosomal protein 131 (CEP131), thereby promoting lysine demethylase 3A (KDM3A) transcription (12). Furthermore, ARID3A has been found to elevate metastasis associated lung adenocarcinoma transcript 1 (MALAT1) and non-coding RNA activated by DNA damage expression to regulate E2F

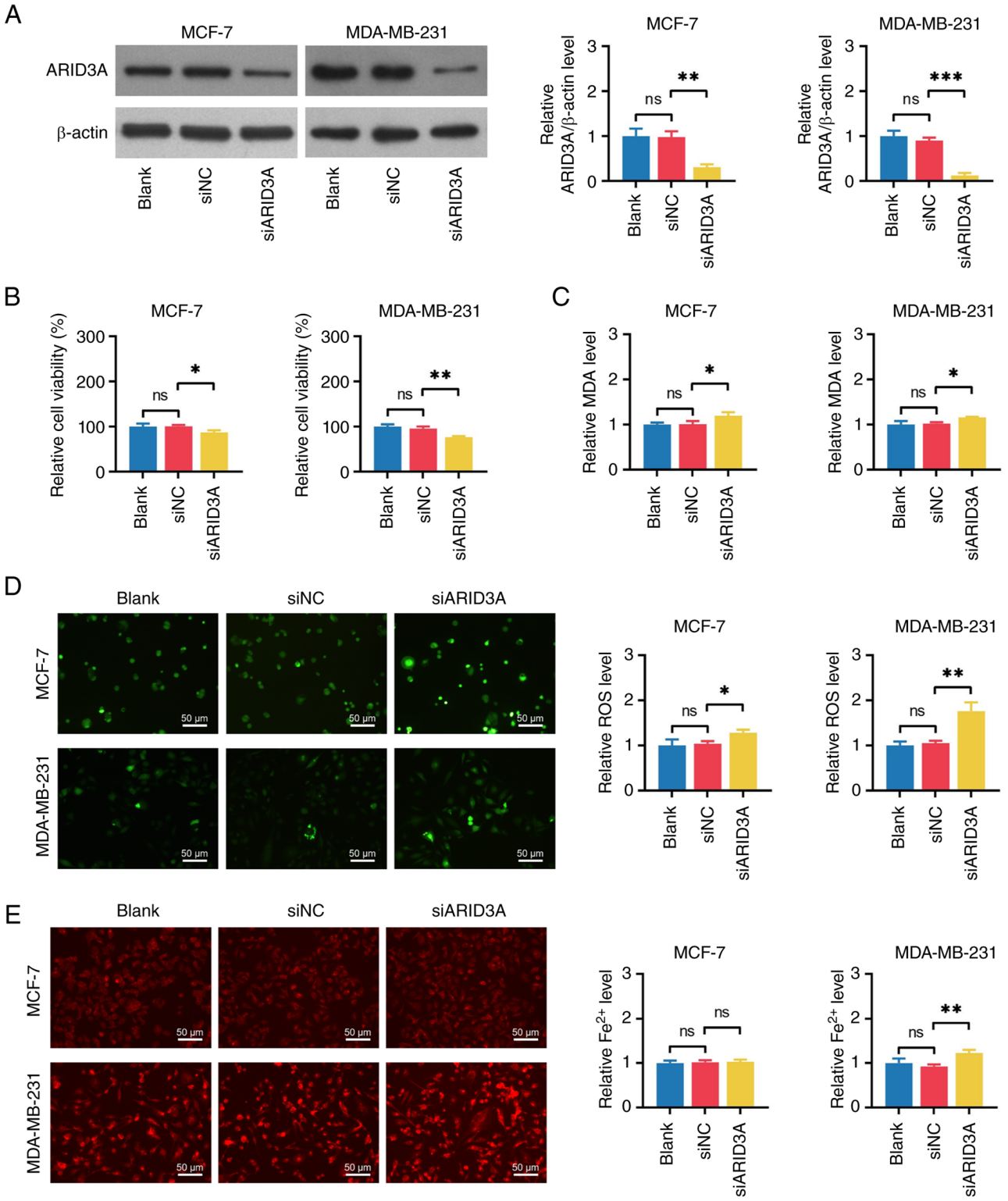

Figure 1. Effect of ARID3A knockdown on cell viability, MDA levels, ROS levels and Fe^{2+} levels. Comparison of (A) ARID3A expression, (B) cell viability, (C) MDA levels, (D) ROS levels and (E) Fe^{2+} levels between the blank group and the siNC group and between the siNC group and the siARID3A group, in breast cancer cell lines. Scale bar, 50 μm. *P<0.05, **P<0.01 and ***P<0.001. ARID3A, AT-rich interaction domain 3A; Fe^{2+}, ferrous iron; MDA, malondialdehyde; NC, negative control; ROS, reactive oxygen species; si, small interfering RNA; ns, not significant.

transcription factor 1 (E2F1) and p53 pathways to induce NSCLC progression (13). However, the association between ARID3A and breast cancer pathogenesis remains unclear. The present study revealed that ARID3A knockdown decreased cell viability in two breast cancer cell lines. The reasons for this may have been: i) ARID3A knockdown repressed oncogenes such as AURKA, CEP131, KDM3A and MALAT1 to reduce breast cancer cell viability (11-13); or ii) ARID3A knockdown regulated carcinogenetic pathways such as E2F1, p53 and Akt to decrease breast cancer cell viability (13,17).

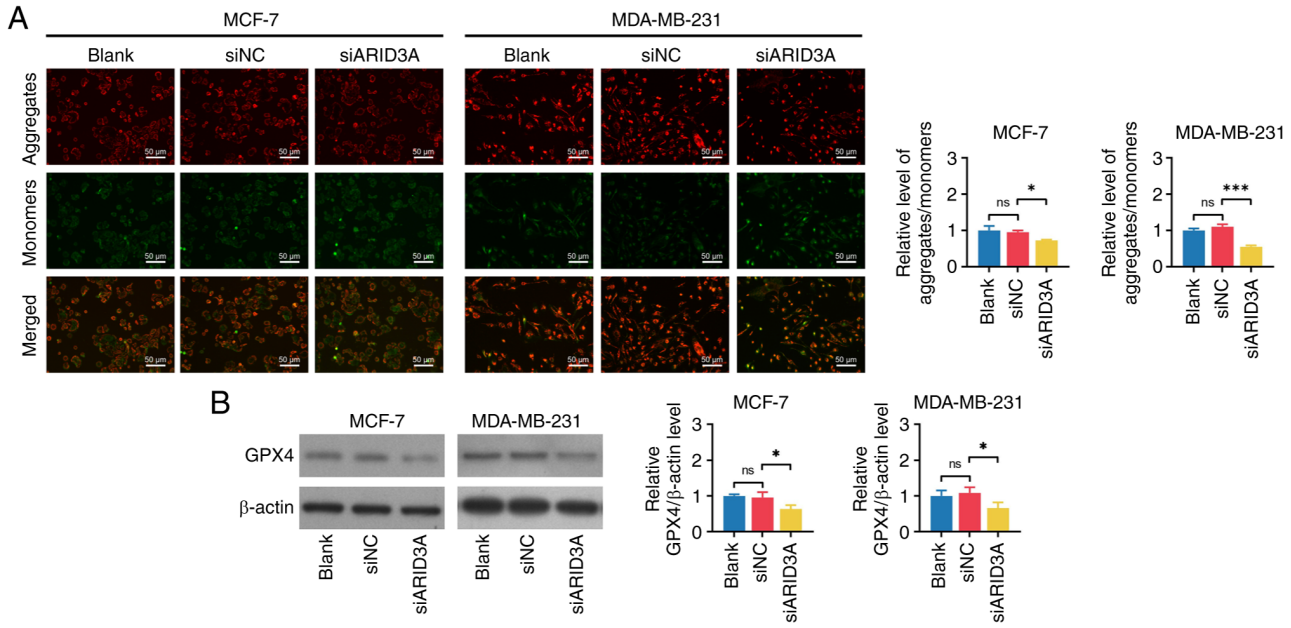

Figure 2. Effect of ARID3A knockdown on the MMP and GPX4 expression. Comparison of (A) the MMP and (B) GPX4 expression between the blank group and the siNC group and between the siNC group and the siARID3A group, in breast cancer cell lines. Scale bar, 50 μm. *P<0.05 and ***P<0.001. ARID3A, AT-rich interaction domain 3A; GPX4, glutathione peroxidase 4; MMP, mitochondrial membrane potential; NC, negative control; si, small interfering RNA; ns, not significant.

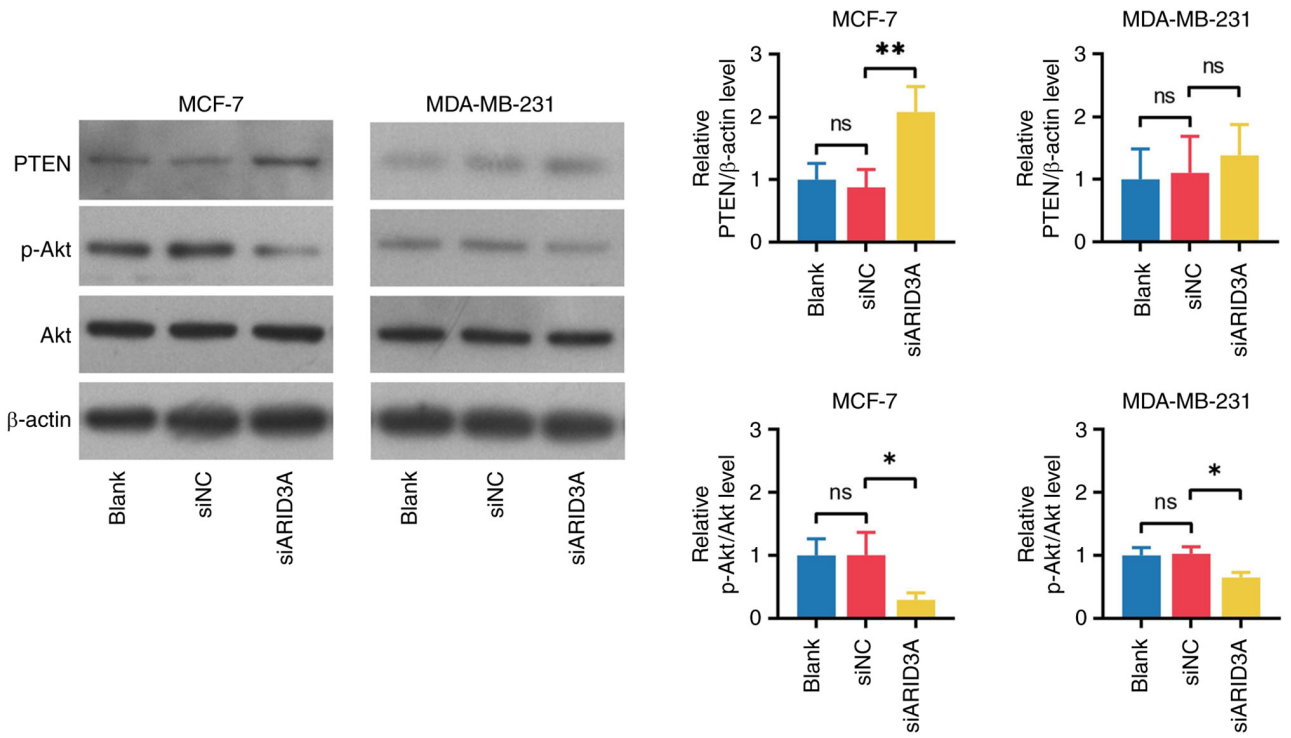

Figure 3. Effect of ARID3A knockdown on the PTEN and Akt pathway. Comparison of PTEN and p-Akt levels between the blank group and the siNC group and between the siNC group and the siARID3A group, in breast cancer cell lines. *P<0.05 and **P<0.01. ARID3A, AT-rich interaction domain 3A; NC, negative control; p-, phosphorylated; si, small interfering RNA; ns, not significant.

Furthermore, two recent studies have reported an association between ARID3A and ferroptosis (17,26), with one revealing that ARID3A induced tumor growth and elevated gemcitabine resistance by repressing PTEN-mediated ferroptosis in pancreatic cancer (17) and the other suggesting that ARID3A may be a ferroptosis signature gene in preeclampsia, based on non-negative matrix factorization clustering and machine learning algorithms (26). However, the association between ARID3A and ferroptosis in breast cancer remains unclear. The present study revealed that ARID3A knockdown promoted ferroptosis in two breast cancer cell lines. The reasons for this may have been: i) ARID3A knockdown upregulated PTEN

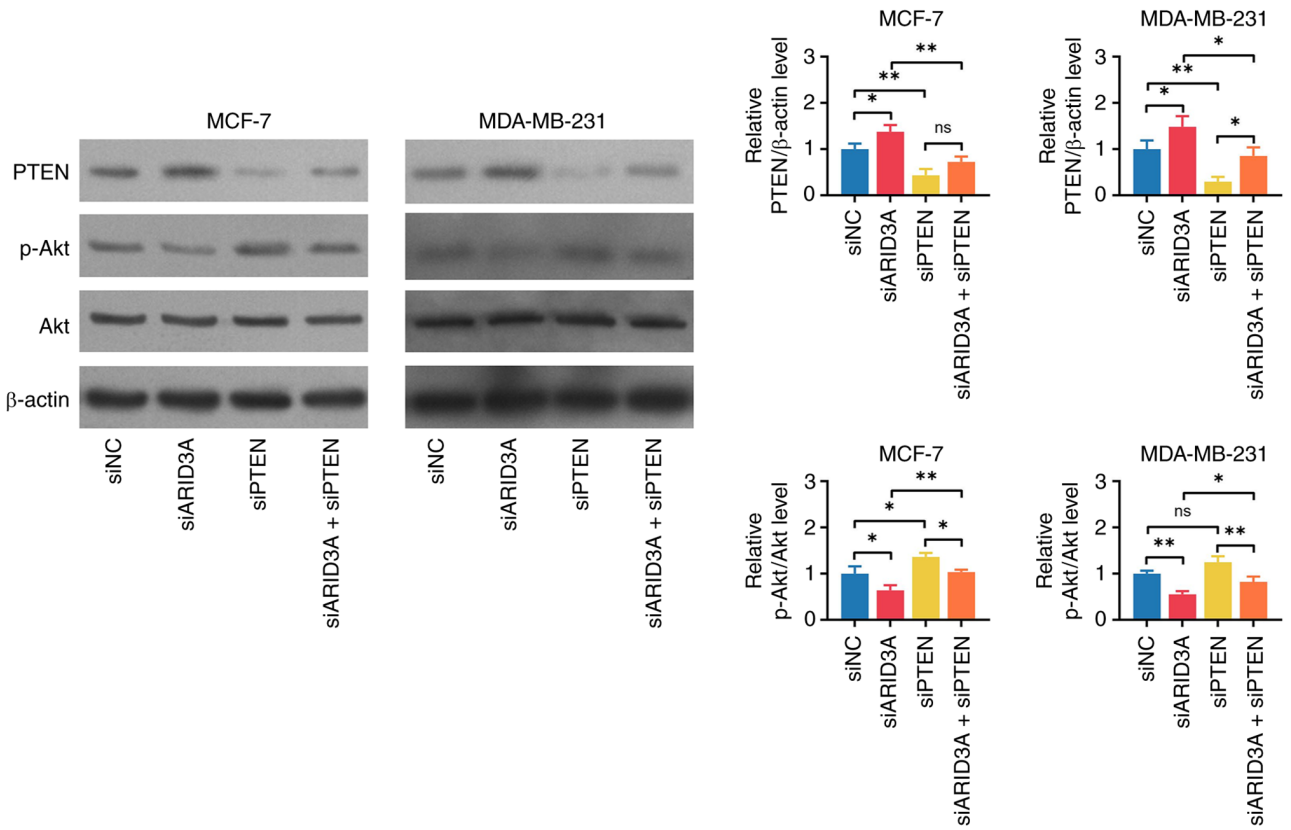

Figure 4. Effect of PTEN knockdown with or without ARID3A knockdown on the Akt pathway. Comparison of PTEN and p-Akt levels among multiple groups, including the siNC, siARID3A, siPTEN and siARID3A + siPTEN groups, in breast cancer cell lines. *P<0.05 and **P<0.01. ARID3A, AT-rich interaction domain 3A; NC, negative control; p-, phosphorylated; si, small interfering RNA; ns, not significant.

to induce ferroptosis (17,22-24); or ii) ARID3A knockdown inactivated the Akt pathway to facilitate ferroptosis (17,25). In the present study, the Fe^{2+} level was significantly increased in MDA-MB-231 cells but not in MCF-7 cells after ARID3A knockdown. This difference may be due to distinct iron-handling characteristics and ferroptosis susceptibility between the two cell lines, including differences in iron uptake, storage and intracellular labile iron homeostasis (27). MCF-7 cells may maintain intracellular iron homeostasis through tighter regulation of iron uptake, sequestration and export, thereby limiting marked changes in the intracellular Fe^{2+} pool following ARID3A knockdown (27) meaning an obvious increase in Fe^{2+} levels was not observed. However, ferroptosis also depends on iron-associated lipid peroxidation rather than increased Fe^{2+} levels alone. In MCF-7 cells, ferroptosis involvement was supported by several findings, including increased ROS and MDA levels indicating enhanced oxidative stress and lipid peroxidation, decreased GPX4 expression suggesting impaired detoxification of lipid peroxides, and the ability of the ferroptosis inhibitor Fer-1 to partially rescue cell injury, collectively supporting ferroptotic cell death despite the absence of a marked Fe^{2+} increase. However, it should be noted that decreased MMP is not a specific hallmark of ferroptosis and is more frequently associated with apoptosis (28).

In the present study, MMP was evaluated as an indicator of mitochondrial dysfunction. Under ferroptotic stress, progressive lipid peroxidation may impair mitochondrial integrity and lead to membrane depolarization. Therefore, the observed MMP reduction should be interpreted as accompanying mitochondrial injury rather than direct evidence of ferroptosis. In addition, the partial rescue effect of Fer-1 further supported that ferroptosis contributed to the phenotype induced by ARID3A knockdown.

PTEN is an established tumor suppressor and relieves treatment resistance in certain cancer types, including breast cancer, melanoma and pancreatic cancer (18,19,29). Specifically, a lack of PTEN systemically enhances tumor growth and the metastatic potential through activation of the Akt pathway in breast cancer (30). PTEN overexpression has also been shown to reduce cell proliferation and induce apoptosis through Akt signaling inactivation in breast cancer (31). Furthermore, PTEN facilitates ferroptosis by inactivating the Akt pathway in numerous cancer types such as pancreatic cancer, NSCLC and melanoma (17,23,32); however, there is a lack of evidence regarding the association between PTEN and ferroptosis in breast cancer. The present study revealed that PTEN knockdown repressed ferroptosis and attenuated the effect of ARID3A knockdown on ferroptosis in two breast cancer cell lines. This may be due to PTEN inactivating the Akt signaling pathway (20,21), which is key in the regulation of ferroptosis in breast cancer (33). The present study primarily demonstrated that ARID3A knockdown was associated with altered PTEN/Akt signaling, but the direct mechanism by which ARID3A regulates PTEN was not investigated. Given that ARID3A is a DNA-binding transcription factor, it may regulate PTEN transcriptionally or influence PTEN through

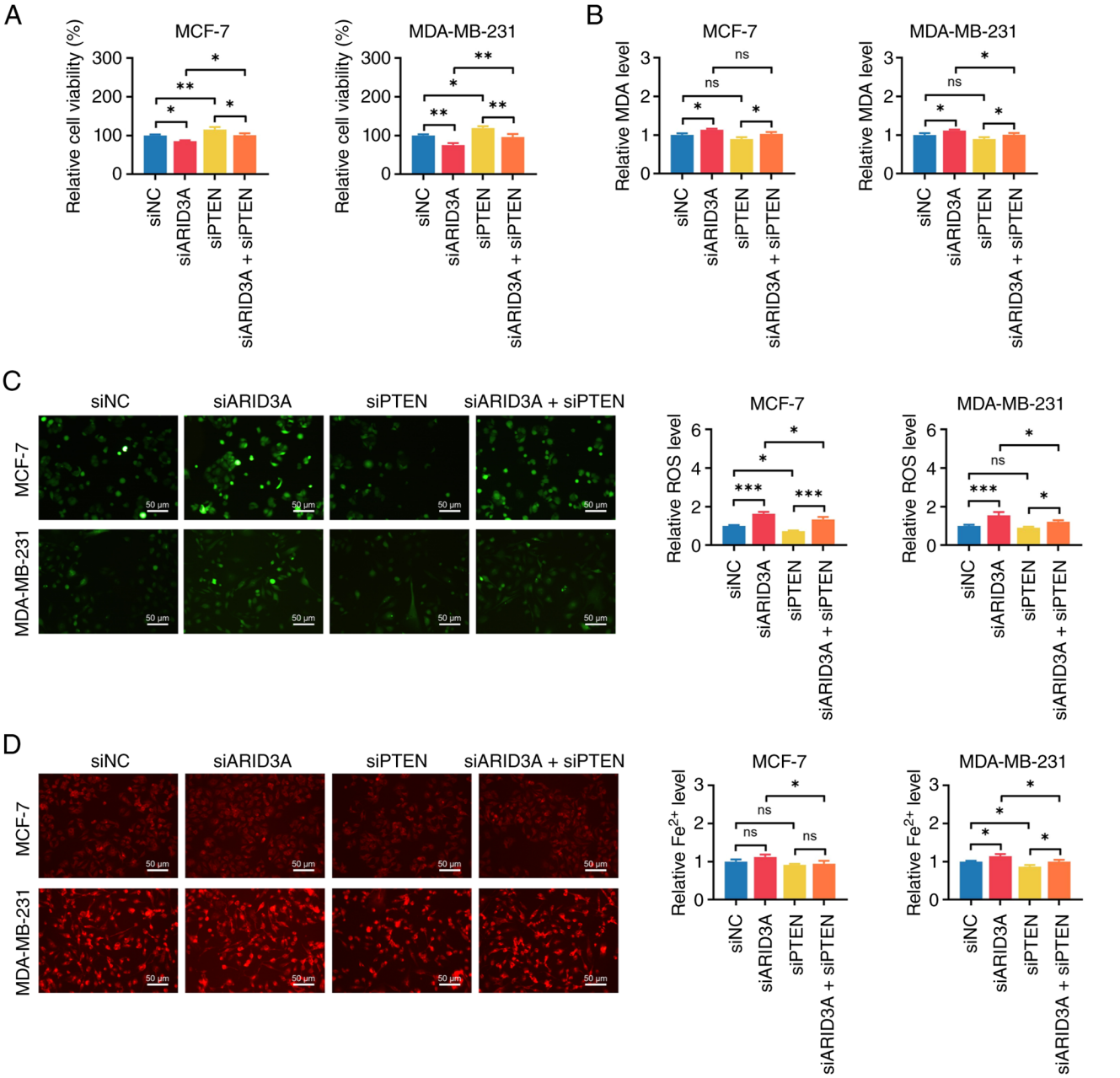

Figure 5. Effect of PTEN knockdown with or without ARID3A knockdown on cell viability, MDA levels, ROS levels and Fe^{2+} levels. Comparison of (A) cell viability, (B) MDA levels, (C) ROS levels and (D) Fe^{2+} levels among numerous groups, including the siNC, siARID3A, siPTEN and siARID3A + siPTEN groups, in breast cancer cell lines. Scale bar, 50 μm. *P<0.05, **P<0.01 and ***P<0.001. ARID3A, AT-rich interaction domain 3A; Fe^{2+}, ferrous iron; MDA, malondialdehyde; NC, negative control; ROS, reactive oxygen species; si, small interfering RNA; ns, not significant.

indirect mechanisms. Previous evidence has shown that ARID3A can repress PTEN transcription through promoter binding in tumor cells (17). Whether a similar mechanism exists in breast cancer requires further validation, perhaps by chromatin immunoprecipitation-quantitative PCR, luciferase reporter assays or protein stability analyses. Notably, in the present study, differential responses were observed between MCF-7 and MDA-MB-231 cells. In MDA-MB-231 cells, ARID3A knockdown did not significantly increase PTEN expression in the initial assay, although an upward trend was detected. In addition, PTEN knockdown alone did not significantly elevate basal p-Akt levels, but it partially reversed the suppression of Akt phosphorylation induced by ARID3A knockdown. These findings indicated that PTEN may function as a conditional regulator rather than the dominant determinant of basal Akt signaling in this cell line. The aggressive molecular background of MDA-MB-231 cells and constitutive activation of parallel pathways, such as MAPK/ERK and STAT3 signaling, may contribute to this phenomenon (34,35). Therefore, the regulation of Akt signaling by ARID3A appears to be cell-context dependent and may involve both PTEN-dependent and PTEN-independent mechanisms depending on cellular context. Although PTEN knockdown partly reversed the effects of ARID3A knockdown in the present study, not all analyses reached statistical significance, suggesting that PTEN may not be the only mediator involved.

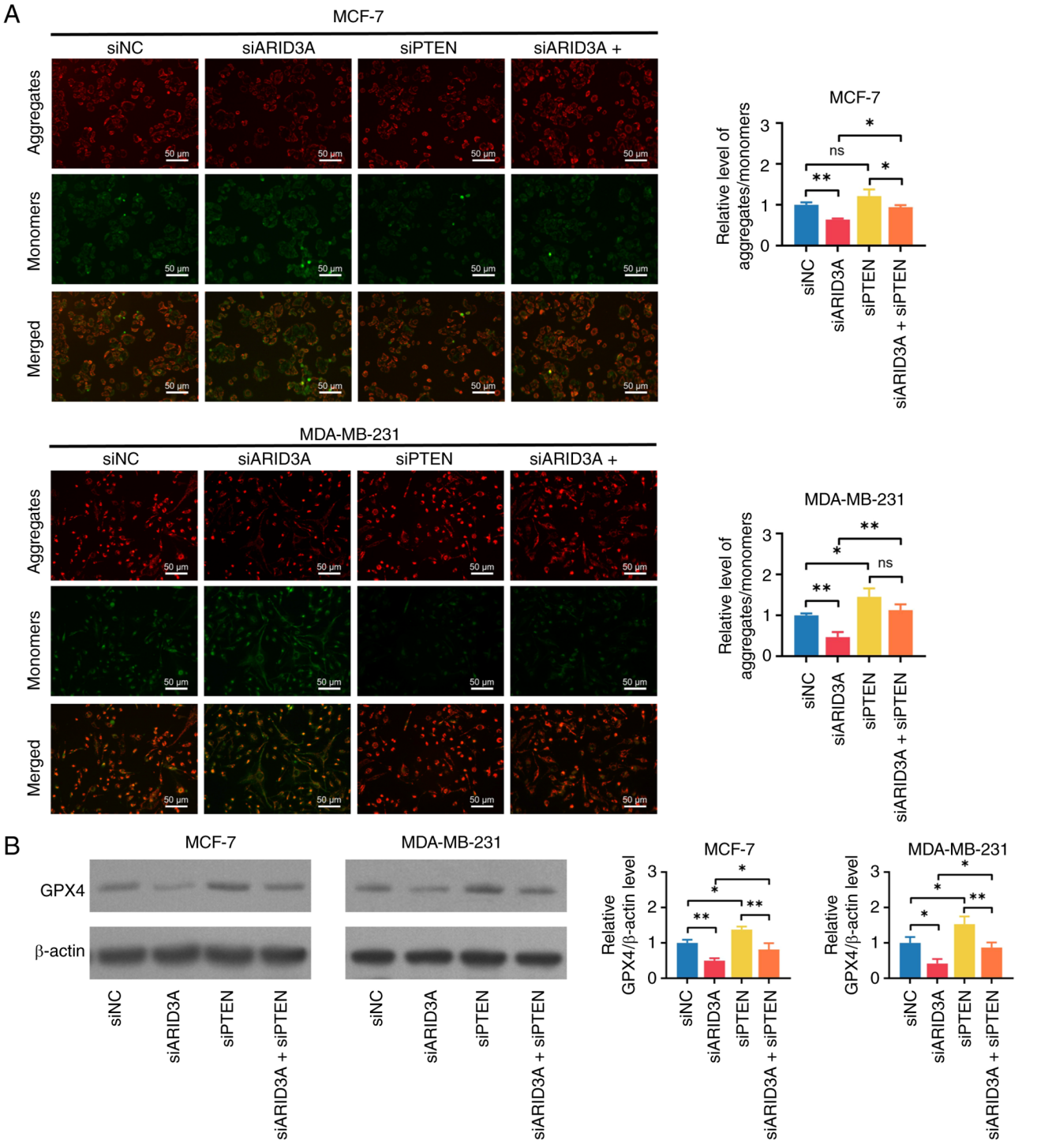

Figure 6. Effect of PTEN knockdown with or without ARID3A knockdown on the MMP and GPX4 expression. Comparison of (A) the MMP and (B) GPX4 expression among numerous groups, including the siNC, siARID3A, siPTEN and siARID3A + siPTEN groups, in breast cancer cell lines. Scale bar, 50 μm. *P<0.05 and **P<0.01. ARID3A, AT-rich interaction domain 3A; GPX4, glutathione peroxidase 4; MMP, mitochondrial membrane potential; NC, negative control; si, small interfering RNA; ns, not significant.

The Akt pathway serves as a central regulator of numerous oncogenic processes in breast cancer, governing cell proliferation, survival, motility and neovascularization (36,37). Its frequent dysregulation through PTEN inactivation, PI3K hyperactivation or Akt amplification has positioned this pathway as a high-priority therapeutic target, driving the development of numerous molecular inhibitors currently under investigation (37,38). Notably, the distinct molecular alterations within this pathway across different breast cancer subtypes underscore the need for precision medicine approaches in targeting Akt signaling (39). In addition, the Akt pathway is a key regulator of ferroptosis in breast cancer (33). The present study demonstrated that PTEN-mediated Akt signaling inactivation was involved in ARID3A knockdown-induced ferroptosis in breast cancer, providing novel evidence regarding the mechanism of ferroptosis regulation by ARID3A in breast cancer.

The present study exhibited a number of limitations that should be acknowledged. Firstly, the upstream molecular mechanism that links ARID3A with PTEN regulation was not fully explored. In addition, varying molecular subtypes of breast cancer may have different signaling backgrounds, which could influence the function of ARID3A. Furthermore, MCF-7 cells are estrogen receptor-positive/HER2-negative, whereas MDA-MB-231 cells are triple-negative. Therefore, differences observed between the two cell lines in the present study may be associated with subtype characteristics. However, the present study did not specifically evaluate the effect of ER or HER2 status on ARID3A function. Further studies using HER2-positive and other subtype models are therefore needed.

In conclusion, ARID3A knockdown facilitated ferroptosis partly by regulating the PTEN-associated Akt pathway in breast cancer. These findings may provide new insight into ferroptosis-based therapeutic strategies for breast cancer. Despite this, further validation is still needed in future studies.

Acknowledgements

Not applicable.

Funding

The present study was supported by the Natural Science Foundation of Hubei Province (grant nos. 2023AFB1023 and 2019CFB124) and the China Primary Health Care Foundation (grant no. cphcf-2023-111).

Availability of data and materials

The data generated in the present study may be requested from the corresponding author.

Authors' contributions

PS and JZ designed the research. YY, MZ, YL and MJ performed the experiments and data acquisition. PS performed the data analysis. All authors wrote and revised the manuscript. PS and JZ confirm the authenticity of all the raw data. All authors read and approved the final version of the manuscript.

Ethics approval and consent to participate

Not applicable.

Patient consent for publication

Not applicable.

Competing interests

The authors declare that they have no competing interests.

References

1. Bray F, Laversanne M, Sung H, Ferlay J, Siegel RL, Soerjomataram I and Jemal A: Global cancer statistics 2022: GLOBOCAN estimates of incidence and mortality worldwide for 36 cancers in 185 countries. CA Cancer J Clin 74: 229-263, 2024.
2. Xiong X, Zheng LW, Ding Y, Chen YF, Cai YW, Wang LP, Huang L, Liu CC, Shao ZM and Yu KD: Breast cancer: Pathogenesis and treatments. Signal Transduct Target Ther 10: 49, 2025.
3. Popa MT, Nodiţi A, Peleaşă TM, Stoleru S and Blidaru A: Breast cancer: A heterogeneous pathology. Prognostic and predictive factors-a narrative review. Chirurgia (Bucur) 120: 32-47, 2025.
4. Díaz O, Rodríguez-Ruíz A and Sechopoulos I: Artificial intelligence for breast cancer detection: Technology, challenges, and prospects. Eur J Radiol 175: 111457, 2024.
5. Carvalho E, Canberk S, Schmitt F and Vale N: Molecular subtypes and mechanisms of breast cancer: Precision medicine approaches for targeted therapies. Cancers (Basel) 17: 1102, 2025.
6. Wang Y, Tang C, Wang K, Zhang X, Zhang L, Xiao X, Lin H and Xiong L: The role of ferroptosis in breast cancer: Tumor progression, immune microenvironment interactions and therapeutic interventions. Eur J Pharmacol 996: 177561, 2025.
7. Wang B, Liu ZH, Li JJ, Xu JX, Guo YM, Zhang JX, Chu T, Feng ZF, Jiang QY and Wu DD: Role of ferroptosis in breast cancer: Molecular mechanisms and therapeutic interventions. Cell Signal 134: 111869, 2025.
8. Zhang S, Guo L, Tao R and Liu S: Ferroptosis-targeting drugs in breast cancer. J Drug Target 33: 42-59, 2025.
9. Peng C, Chen Y and Jiang M: Targeting ferroptosis: A promising strategy to overcome drug resistance in breast cancer. Front Oncol 14: 1499125, 2024.
10. Liu G, Huang YJ, Xiao R, Wang D, Acton TB and Montelione GT: Solution NMR structure of the ARID domain of human AT-rich interactive domain-containing protein 3A: A human cancer protein interaction network target. Proteins 78: 2170-2175, 2010.
11. Tang J, Yang L, Li Y, Ning X, Chaulagain A, Wang T and Wang D: ARID3A promotes the development of colorectal cancer by upregulating AURKA. Carcinogenesis 42: 578-586, 2021.
12. Shen M, Li S, Zhao Y, Liu Y, Liu Z, Huan L, Qiao Y, Wang L, Han L, Chen Z and He X: Hepatic ARID3A facilitates liver cancer malignancy by cooperating with CEP131 to regulate an embryonic stem cell-like gene signature. Cell Death Dis 13: 732, 2022.
13. Nasuh S, Balci SO, Bozgeyik I, Ikeda MA, Tekayev M and Saadat KASM: ARID3A and ARID3B exert direct regulatory control over the long non-coding RNAs (lncRNAs) MALAT1 and NORAD within the context of non-small cell lung cancer (NSCLC). Pathol Res Pract 252: 154948, 2023.
14. Zhang DY, Zhu Y, Ma SS, Xu CY, Wang ZL, Wang H, Liu SH, Shang J, Huang XL, Malgulwar PB, *et al*: Phosphorylation enhanced OTUD3 deubiquitination ARID3A promotes the progress of cholangiocarcinoma. Oncogene 44: 2040-2053, 2025.
15. Cai WR, Sun XG, Yu Y, Wang X, Cao XC and Liu XF: Unveiling the prognostic value of ARID3A in breast cancer through bioinformatic analysis. Heliyon 11: e42024, 2025.
16. Kang Y, Zhu X, Wang X, Liao S, Jin M, Zhang L, Wu X, Zhao T, Zhang J, Lv J and Zhu D: Identification and validation of the prognostic stemness biomarkers in bladder cancer bone metastasis. Front Oncol 11: 641184, 2021.
17. Mao X, Xu J, Xiao M, Liang C, Hua J, Liu J, Wang W, Yu X, Meng Q and Shi S: ARID3A enhances chemoresistance of pancreatic cancer via inhibiting PTEN-induced ferroptosis. Redox Biol 73: 103200, 2024.
18. Liu J, Pan Y, Liu Y, Wei W, Hu X, Xin W and Chen N: The regulation of PTEN: Novel insights into functions as cancer biomarkers and therapeutic targets. J Cell Physiol 238: 1693-1715, 2023.
19. Maphutha J, Twilley D and Lall N: The role of the PTEN tumor suppressor gene and its anti-angiogenic activity in melanoma and other cancers. Molecules 29: 721, 2024.
20. Sadrkhanloo M, Paskeh MDA, Hashemi M, Raesi R, Bahonar A, Nakhaee Z, Entezari M, Beig Goharrizi MAS, Salimimoghadam S, Ren J, *et al*: New emerging targets in osteosarcoma therapy: PTEN and PI3K/Akt crosstalk in carcinogenesis. Pathol Res Pract 251: 154902, 2023.
21. Parsons R: Discovery of the PTEN tumor suppressor and its connection to the PI3K and AKT oncogenes. Cold Spring Harb Perspect Med 10: a036129, 2020.
22. Pan R, Zhao Z, Xu D, Li C and Xia Q: GPX4 transcriptionally promotes liver cancer metastasis via GRHL3/PTEN/PI3K/AKT axis. Transl Res 271: 79-92, 2024.

23. Wu B, Li D, Wang Y, Pan T, Xu J and Li L: The m6A methyltransferase METTL3 affects ferroptosis in non-small cell lung cancer by regulating the PTEN/PI3K/AKT pathway. Discov Oncol 16: 559, 2025.
24. Cahuzac KM, Lubin A, Bosch K, Stokes N, Shoenfeld SM, Zhou R, Lemon H, Asara J and Parsons RE: AKT activation because of PTEN loss upregulates xCT via GSK3β/NRF2, leading to inhibition of ferroptosis in PTEN-mutant tumor cells. Cell Rep 42: 112536, 2023.
25. Su H, Peng C and Liu Y: Regulation of ferroptosis by PI3K/Akt signaling pathway: A promising therapeutic axis in cancer. Front Cell Dev Biol 12: 1372330, 2024.
26. Liu X, Zhang D and Qiu H: NMF typing and machine learning algorithm-based exploration of preeclampsia-related mechanisms on ferroptosis signature genes. Cell Biol Toxicol 41: 14, 2024.
27. Bajbouj K, Shafarin J and Hamad M: High-Dose deferoxamine treatment disrupts intracellular iron homeostasis, reduces growth, and induces apoptosis in metastatic and nonmetastatic breast cancer cell lines. Technol Cancer Res Treat 17: 1533033818764470, 2018.
28. Dixon SJ and Olzmann JA: The cell biology of ferroptosis. Nat Rev Mol Cell Biol 25: 424-442, 2024.
29. Tufail M: PTEN-mediated resistance in cancer: From foundation to future therapies. Toxicol Rep 14: 101987, 2025.
30. Chen J, Sun J, Wang Q, Du Y, Cheng J, Yi J, Xie B, Jin S, Chen G, Wang L, *et al*: Systemic deficiency of PTEN accelerates breast cancer growth and metastasis. Front Oncol 12: 825484, 2022.
31. Zhang J, Zhang Y, Lin X, Han X, Meredith KL and Li Z: The effects of the tumor suppressor gene PTEN on the proliferation and apoptosis of breast cancer cells via AKT phosphorylation. Transl Cancer Res 12: 1863-1872, 2023.
32. Sun H, Meng Y, Yao L, Du S, Li Y, Zhou Q, Liu Y, Dian Y, Sun Y, Wang X, *et al*: Ubiquitin-specific protease 22 controls melanoma metastasis and vulnerability to ferroptosis through targeting SIRT1/PTEN/PI3K signaling. MedComm (2020) 5: e684, 2024.
33. Pandey P, Pandey S, Ramniwas S, Ballal S, Kumar S, Bhat M, Sharma S, Kumar MR and Khan F: A review unveiling the ferroptosis-regulated cell signalling pathways in breast cancer to elucidate potent targets for cancer management. Curr Pharm Des 31: 1593-1603, 2025.
34. Mirzoeva OK, Das D, Heiser LM, Bhattacharya S, Siwak D, Gendelman R, Bayani N, Wang NJ, Neve RM, Guan Y, *et al*: Basal subtype and MAPK/ERK kinase (MEK)-phosphoinositide 3-kinase feedback signaling determine susceptibility of breast cancer cells to MEK inhibition. Cancer Res 69: 565-572, 2009.
35. Banerjee K and Resat H: Constitutive activation of STAT3 in breast cancer cells: A review. Int J Cancer 138: 2570-2578, 2016.
36. Wali AF, Talath S, El Tanani M, Rashid Rangraze I, Babiker R, Shafi S and Bansal R: PI3K/AKT/mTOR pathway in breast cancer pathogenesis and therapy: Insights into phytochemical-based therapeutics. Nutr Cancer 77: 938-958, 2025.
37. Khorasani ABS, Hafezi N, Sanaei MJ, Jafari-Raddani F, Pourbagheri-Sigaroodi A and Bashash D: The PI3K/AKT/mTOR signaling pathway in breast cancer: Review of clinical trials and latest advances. Cell Biochem Funct 42: e3998, 2024.
38. Luboff AJ and DeRemer DL: Capivasertib: A Novel AKT inhibitor approved for hormone-receptor-positive, HER-2-Negative metastatic breast cancer. Ann Pharmacother 58: 1229-1237, 2024.
39. Zhu K, Wu Y, He P, Fan Y, Zhong X, Zheng H and Luo T: PI3K/AKT/mTOR-targeted therapy for breast cancer. Cells 11: 2508, 2022.